

## Synthesis of polyaniline/nanosilica nanocomposite for removal of reactive orange 16 from aqueous solutions

Habib-Allah Tayebi\*

Department of Textile Engineering, Qaemshahr Branch, Islamic Azad University, Qaemshahr, Iran.

Received: November 2015; Revised: December 2015; Accepted: January 2016

**Abstract:** In this study, preparation of polyaniline (PAni) and its nanocomposite containing nanosilica (NS) was discussed, and their capability to removal of reactive orange 16 (RO16) from aqueous solution was studied. Polyaniline (PAni) synthesized chemically in the presence of potassium iodate ( $\text{KIO}_3$ ) as an oxidant and coated on nanosilica. The removal of RO16 was investigated using PAni, and PAni/NS nanocomposite, respectively. The products were investigated in terms of morphology and chemical structure with scanning electron microscopy (SEM), and Fourier-transform infrared spectroscopy (FTIR), respectively. Batch studies were performed to evaluate the influence of various experimental parameters like pH, adsorbent dosage and contact time. Optimum conditions for RO16 removal were found to be pH 2, adsorbent dosage of 0.8 g/L, equilibrium time 150 min. For determining the type of adsorption isotherm, Langmuir and Freundlich adsorption isotherms were used. The results revealed that Langmuir isotherm adequately met the experimental requirements. According to the Langmuir model, polyaniline/silica nano composite sorbents exhibited the highest RO 16 dye adsorption capacity of 60.98 mg  $\text{g}^{-1}$ . Thermodynamic parameters such as changes in Gibbs free energy ( $\Delta G^\circ$ ), enthalpy ( $\Delta H^\circ$ ) and entropy ( $\Delta S^\circ$ ) were calculated. The negative values of  $\Delta G^\circ$  and the positive value of  $\Delta H^\circ$  (24.49 KJ/mol) and  $\Delta S^\circ$  (97.11 J/mol K) show that the RO 16 adsorption on polyaniline/silica nanocomposite was a spontaneous and endothermic process.

**Keywords:** Nanocomposite, Nanosilica, Polyaniline, Reactive orange 16, Removal.

### Introduction

Dyes are widely used in various fields of industrial applications such as textile and their discharge into water causes environmental pollution [1]. Among all forms of dyes, azoic dyes which are complex aromatic structures resist highly to biodegradation [2]. Reactive Orange 16 is a water-soluble azo dye which is difficult to be removed from waste water. The treatment of dye-contaminated wastewater is one of the most serious environmental problems faced by the textile. To minimize the risk of pollution generated by such effluent, this effluent must be treated before discharged

into the environment. There are several methods for removing dyes and other color contaminants: aerobic/anaerobic biological degradation, chemical coagulation, membrane filtration, flocculation, photochemical degradation and chemical oxidation. These methods are not economical and none of them are able to totally remove dyes from waste water [3-6]. Among these methods, adsorption has now become popular because of its easy operations and low running costs [7, 8]. Several adsorbents have been developed for the purification of waste water including zeolite (synthesized from coal fly ash) [9], SBA-15/poly pyrrole nanocomposite [10], poly aniline/Activated carbon composite [11]. PAni, as one of the most potentially useful conducting polymers, has recently

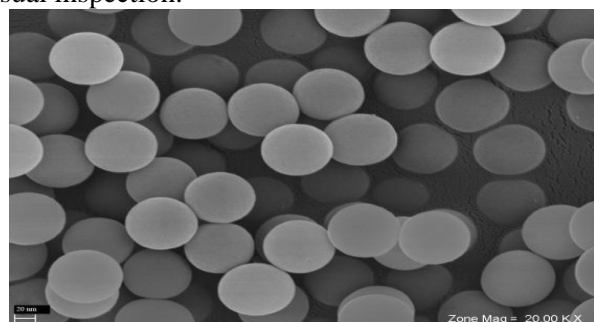
\*Corresponding author. Tel: (+98) 9112160238, Fax: (+98) 11 32535104, E-mail: tayebi\_h@yahoo.com

received considerable attention, because of the low cost of its monomer [11-14]. PANi is a poly aromatic amine that can be easily synthesized chemically from bronsted acidic aqueous solutions [11, 14-17]. Chemical polymerization of aniline in aqueous acidic solutions can be performed through using oxidizing agents such as  $\text{KIO}_3$ . Nano materials represent remarkable advantages due to their unique properties. In recent years, using nanoparticles in many fields, such as in protein separation [18-20], removal of metal ions and dyes [21-23], biotechnology and biomedicine has had many pros because of their unique properties including the large surface area and small diffusion resistance [24-29]. In this article, PANi/NS nanocomposite is synthesized, characterized and applied to study adsorption capacity of RO 16 from aqueous solution by achieving optimum experimental conditions.

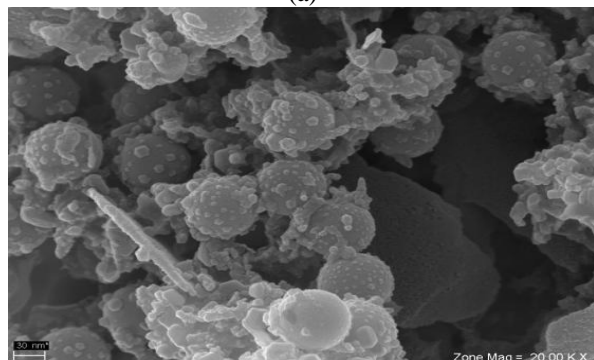
## Results and discussion

### Surface morphology:

The morphology of Nano silica before and after coating with PANi is illustrated in Figures 1a and 1b. The coating with conducting polymer produced by surface polymerization is very visible. The coating of Nano silica has always been found to be uniform by visual inspection.



(a)



(b)

**Figure 1:** SEM image of (a) NS and (b) PANi/NS.

### Fourier transform infrared spectroscopy (FTIR):

The structure of obtained product was determined by FTIR spectrum. The FTIR spectroscopy has provided valuable information regarding the formation of polyaniline nanocomposite. FTIR analysis has been done to identify the characteristic peaks of product. FTIR spectra in the  $4000\text{--}400\text{ cm}^{-1}$  region, as can be seen in Figure 2, PANi shows the presence of characteristic absorption bands at  $1560\text{ cm}^{-1}$  (C=C stretching vibration of the quinoid ring),  $1500\text{ cm}^{-1}$  (stretching vibration of C=C of the benzenoid ring),  $1308\text{ cm}^{-1}$  (C-N stretching vibration),  $1124\text{ cm}^{-1}$  (C-H in-plane deformation) and  $860\text{ cm}^{-1}$  (C-H out of-plane deformation) [30]. The peak at  $1642\text{ cm}^{-1}$  is attributed to the bending vibration of the O-H bonds in adsorbed water molecule on the surface of nanosilica. The peak at  $1124\text{ cm}^{-1}$  is assigned to Si-O-Si asymmetric stretching vibration and the band at  $800\text{ cm}^{-1}$  is due to the symmetric stretching vibration of the Si-O-Si bond. The peak appeared at  $500\text{ cm}^{-1}$  is related to bending vibration peak of the Si-O-Si bond [31].

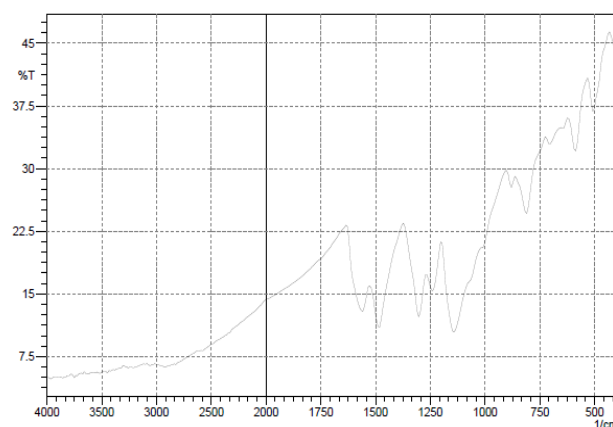


**Figure 2:** FTIR pattern of PANi/NS nanocomposite.

### Effect of pH:

The pH value of the aqueous solution is an important controlling parameter in the adsorption process. These pH values affect the surface charge of adsorbent during adsorption. In order to evaluate the influence of this parameter on the adsorption, the experiments were carried out at different initial pH ranging from 2 to 12. The experiment was performed by PANi and PANi/NS nano composite, with an initial concentration of  $20\text{ mg/l}$ , at room temperature with contact time of 120 min. The results are shown in Figure 3. Removal of RO 16 increases with decreasing pH and a maximum value was reached at an equilibrium pH of around 2, as can be seen in Figure 3. This happened because in acidic

environments, the amino groups of Polymer Polyaniline ( $-NH_2$ ) are protonated in the presence of the released  $H^+$  Protons in the environment; therefore, the adsorption of RO 16, which has a negative charge, increases. With protonation of the adsorption surface, the tendency of RO 16 to the adsorption surface increases. In comparison with the adsorption of Polyaniline, Polyaniline composite adsorbs more dye because of the tiny size of the NS nanoparticles (about 80 nm). With the placement of Polymer nanoparticles of Polyaniline on the composite, more amino groups of Polyaniline were available. Thus, more dye was adsorbed on the composite.

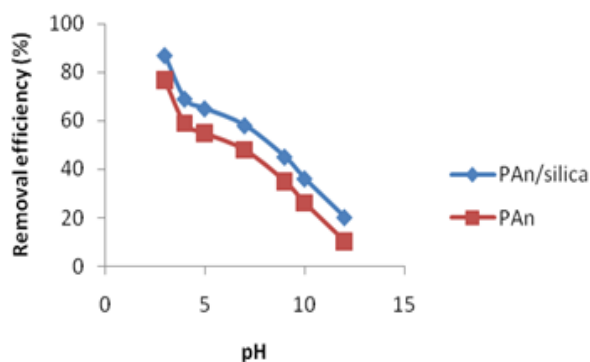


**Figure 3:** The effect of pH on the removal efficiency with: PAni/NS, PAni (The initial concentration, contact time, volume of solution and amount of adsorbent was 20 mg/L, 120 min, 100 mL and 0.1 g, respectively).

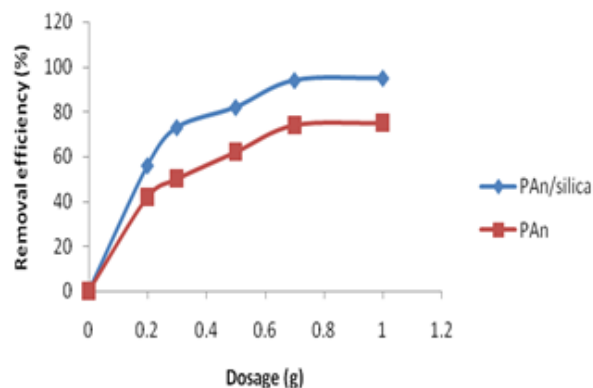
#### Influence of sorbent dosage:

The removal percentage of RO 16 was studied by varying the adsorbent (PAni and PAni/NS) dose between 100 and 1000 mg/L at dye concentration of 20 mg/L. Results are presented in Figure 4. The RO 16 removal efficiency increases up to an optimum dosage beyond which the removal efficiency does not significantly change. This result was anticipated because for a fixed initial solute concentration, increasing adsorbent doses provides greater surface area and more adsorption sites, whereas the adsorbed RO 16 quantity per unit weight of the sorbent decreased by increasing the adsorbent quantity. At very low adsorbent concentration, the adsorbent surfaces become saturated with the dye and the residual dye concentration in the solution was high.

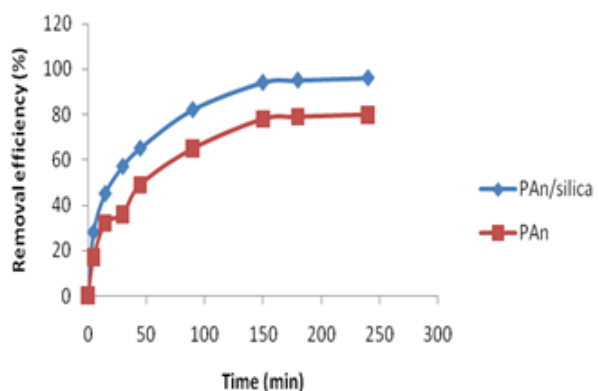
#### Effect of contact time:

Figure 5 shows the effect of contact time on sorption of RO 16 by PAni and PAni/NS. For these cases, initial dye concentration was 20 mg/L and pH of 2 was used

for dye solution. Also PAni and PAni/NS dose of 0.1 g in 100 mL were used. For dye sorption rate reaches up to 80 and 94 by PAni and PAni/NS, respectively, when contact time was 150 min, and then little change of sorption rate was observed. This result revealed that adsorption of RO 16 was fast at first (until 100 min) and the equilibrium was achieved after 150 min of contact time. Taking into account these results, a contact time of 150 min was chosen for further experiments.



**Figure 4:** The effect of adsorbent dosage on the removal efficiency with: PAni/NS and PAni (the initial concentration, pH, contact time and volume of solution was 20 mg/L, 2, 120 min and 100 mL, respectively).



**Figure 5:** The effect of contact time on the removal efficiency with: PAni/NS and PAni (the initial concentration, pH, volume of solution and amount of adsorbent was 20 mg/L, 2, 100 mL and 0.1 g, respectively).

#### Adsorption Isotherms:

Appropriate correlations in the equilibrium data have fundamental importance in the design of an adsorption system for removing dyes. In the present study, three isotherm models have been tested for treatments of the equilibrium adsorption data.

**Langmuir Isotherm Model:**

Langmuir theory was based on the assumption that the uptake of adsorbate occurs on a homogeneous surface by monolayer adsorption and adsorption energy is constant in this model. The theory can be represented by the following equation:

$$q_e = \frac{q_m k_L c_e}{1 + k_L c_e} \quad (1)$$

Where  $q_e$  is the quantity of dye adsorbed (mg/g) at equilibrium,  $C_e$  is the equilibrium dye concentrations in residual dyeing bath (mg/l) and  $k_L$  (l/mg) and  $q_m$  (mg/g) are the Langmuir constants. Table 1 shows that the Langmuir isotherm model could be linearized to at least four different types [32]. The Langmuir constants  $k_L$ , and  $q_m$  values can be calculated from the plot between  $C_e/q_e$  versus  $C_e$ ,  $1/q_e$  versus  $1/C_e$ ,  $q_e$  versus  $q_e/C_e$ , and  $q_e/C_e$  versus  $q_e$  for type 1, type 2, type 3, and type 4 Langmuir isotherms, respectively.

Table 2 shows the predicted isotherm constants ( $k_L$  and  $q_m$ ) and the corresponding  $R^2$  values. The isotherm parameters obtained from the four linearized Langmuir

isotherms were different. Type 1 Langmuir isotherm (Figure 6) was found to be the best fitting linearized Langmuir expression with coefficient of determination of approximately 1. Therefore, the results were taken from Langmuir equation type 1. Correlation coefficients are near to 1 which means that experimental data fitted in this model well.

Essential characteristics of the Langmuir type adsorption process can be classified by a term " $R_L$ ", a dimensionless constant separation factor. The  $R_L$  value indicates the favorability and the shape of the isotherms as follows:

$$R_L = \frac{1}{1 + K_L C_0} \quad (2)$$

$R_L$  is a dimensionless constant separation factor,  $C_0$  is the initial concentration of dye solution (mg/L), and  $k_L$  is the Langmuir constant (L/mg), the parameter  $R_L$  indicates the shape of the isotherm accordingly. Table 2 depicts the values of  $R_L$ . The magnitude of the exponent  $R_L$  gives an indication of the favorability of adsorption. According to Table 3, Values of  $0 < R_L < 1$  represent favorable adsorption conditions.

**Table 1:** Langmuir isotherm and its linear forms.

Langmuir Isotherm	Linear form	Plot
Type1	$\frac{C_e}{q_e} = \frac{1}{q_m} c_e + \frac{1}{k_L q_m}$	$C_e/q_e$ vs. $C_e$
Type2	$\frac{1}{q_e} = \frac{1}{k_L q_m c_e} + \frac{1}{k_L q_m}$	$1/q_e$ vs. $1/C_e$
Type 3	$q_e = q_m - \frac{q_e}{k_L c_e}$	$q_e$ vs. $q_e/C_e$
Type4	$\frac{q_e}{c_e} = k_L q_m - k_L q_e$	$q_e/C_e$ vs. $q_e$

**Table 2:** Calculated Langmuir isotherm parameters by different linear method.

Langmuir Adsorption isotherm	Type1	Type2	Type3	Type4
$q_m$	60.98	72.432	59.47	58.24
$K_L$	0.097	0.080	0.093	0.078
$R^2$	0.996	0.962	0.912	0.912
$R_L$	0.094	0.134	0.117	0.123

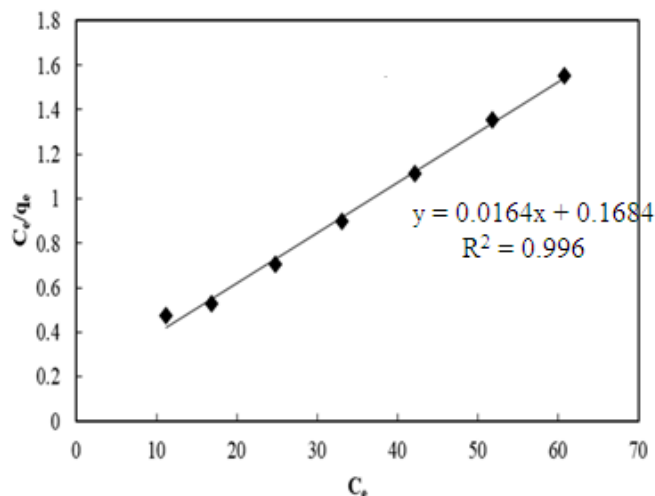


**Figure 6:** Langmuir sorption isotherm of RO 16 onto PANi/NS.

**Table 3:** Values of separation factor  $R_L$ .

Value of $R_L$	Type of isotherm
$R_L > 1$	Unfavorable
$R_L = 1$	Linier
$R_L = 0$	Irreversible
$0 < R_L < 1$	Favorable

#### Freundlich Isotherm Model:

The Freundlich isotherm model equation deals with physicochemical adsorption on heterogeneous surface at sites with different energy of adsorption and with non-identical adsorption sites that are not always available [32]. Mathematically, it is characterized by the heterogeneity factor  $1/n$ .

$$q_e = k_F c_e^{1/n} \quad (3)$$

Where  $K_F$  is the Freundlich constant and  $n$  is the heterogeneity factor. The  $K_F$  value is related to the adsorption capacity, while  $1/n$  value is related to the

adsorption intensity. Freundlich model can be represented by the linear form as follows:

$$\ln q_e = \ln k_F + \frac{1}{n} \ln c_e \quad (4)$$

Therefore,  $K_F$  and  $1/n$  can be determined from the linear plot of  $\ln q_e$  against  $\ln c_e$ . The  $K_F$  and  $n$  values are listed in Table 4. Correlation coefficient is below 0.95 suggesting that experimental data is not fitted to this model. The value of correlation coefficient is lower than the other three isotherms values. The Freundlich isotherm (Figure 7) represents the poorer fit of experimental data than the other isotherms.

**Table 4:** Calculated different isotherm parameters by linear method.

Langmuir Isotherm Model				Freundlich Isotherm Model		
$q_m$	$K_L$	$R_L$	$R^2$	$K_F$	$n$	$R^2$
<b>60.98</b>	0.097	0.094	0.996	9.45	3.11	0.8864

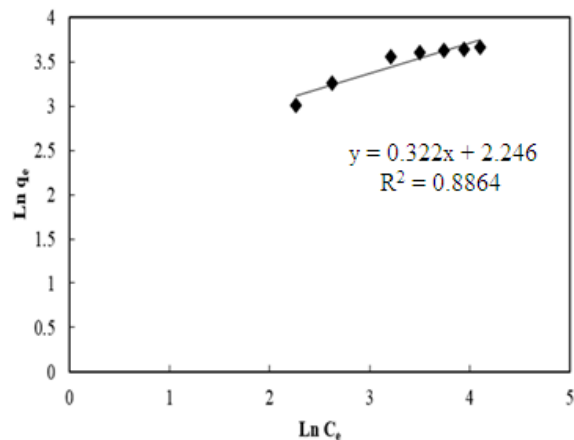
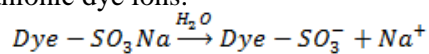


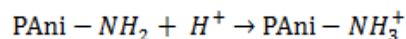
**Figure 7:** Freundlich sorption isotherm of RO 16 onto PAni/NS

#### Adsorption Mechanism:

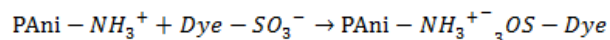
By considering the adsorption of RO 16 onto the surface of PAni/ NS, different mechanisms may be involved such as ionic attraction between anionic sulphonate group(s) of dissolved dye molecules and the cationic amino groups of protonated PAni/ NS. The possible mechanisms of the adsorption process of PAni/ NS and RO 16 is discussed: In aqueous solution, the RO 16 is first dissolved and the sulphonate groups of RO 16 (D-SO<sub>3</sub>Na) is dissociated and converted to anionic dye ions.



Also, in the presence of H<sup>+</sup>, the amino groups of polyaniline (-NH<sub>2</sub>) are protonated.



The adsorption process then proceeds due to the electrostatic attraction between these two counter ions:



#### Thermodynamic parameters:

The Gibbs free energy changes (ΔG°) were determined by using following equation (5):

$$-\Delta G^\circ = RT \ln K \quad (5)$$

Where, R is the gas constant, T is the absolute temperature (K), and K is the partition ratio. The values of partition ratio (K) and Gibbs free energy change (ΔG°) are presented in Table 6. The negative Values of Gibbs free energy change (ΔG°) confirm that the adsorption of RO 16 onto PAni/ NS is spontaneous and thermodynamically favorable. The more negative values of ΔG° imply that the greater driving force is required for the adsorption process. As the temperature

increases, the ΔG° values decrease, indicating less driving force and hence resulting in lesser adsorption capacity at higher temperatures. Standard enthalpy (ΔH°) and entropy (ΔS°) were determined from the Van't Hoff equation [32]:

$$\ln k = \frac{\Delta S^\circ}{R} - \frac{\Delta H^\circ}{RT}$$

(6)

ΔH° and ΔS° were obtained from the slope and intercept of the plot of lnk against 1/T, as shown in Figure 8. The values of ΔH° and ΔS° are listed in Table 5. The value of ΔH° is positive, indicating that the adsorption process is endothermic in nature.

**Table 5:** Thermodynamic Parameters (ΔH°, ΔG°, ΔS°) for the Adsorption of RO 16 on PAni/ NS

Temperature (°C)	K	ΔG°(kJ/mol)	ΔH°(KJ/mol)	ΔS°(J/mol K)	R <sup>2</sup>
25	9.16	-5.49			
35	1.224	-6.41	24.49	97.11	0.994
45	1.632	-7.38			

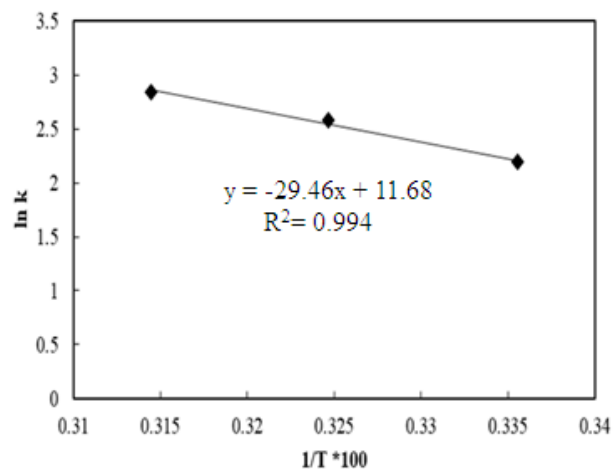


**Figure 8:** Van't Hoff plot for calculated thermodynamic parameter.

#### Conclusion

According to this study, polyaniline/NS nano composite is an effective adsorbent for the removal of Reactive Orange 16 dye from aqueous solution. The maximum removal was observed at a sorbent dose of 0.08 g, contact time of 150 min and pH 2. The

equilibrium adsorption was best fitted with the Langmuir isotherm. The maximum dye adsorption capacity of PANi/NS nano composite obtained from the Langmuir model at 25 °C was 60.98 mg g<sup>-1</sup>. Based on the results obtained from thermodynamic parameters such as enthalpy change ( $\Delta H^\circ$ ), entropy change ( $\Delta S^\circ$ ) and changes in the Gibbs free energy ( $\Delta G^\circ$ ), it was revealed that the adsorption process was endothermic, feasible and spontaneous.

## Experimental

### Materials and equipment:

All chemicals used in this study were analytical reagents grade and prepared in distilled water. Aniline was obtained from Merck and distilled before use. As shown in Figure 9, PANi contain y-reduced (benzenoid diamine) and (1-y) oxidized repeat groups (quinoid diamine) and n is the degree of polymerization. Tetraethoxysilane (TEOS), Hexadecyl Trimethyl Ammonium Bromide (CTAB), acetone, sulfuric acid, hydrochloric acid and sodium hydroxide were used without further purification processes. All of these materials were supplied from Merck. Reactive orange 16 was purchased from Dystar (Figure 10 & Table 6). This dye shows an intense absorption peak in the visible region at 390nm. This wavelength corresponds to the maximum adsorption peak of the Reactive

**Table 6:** Characteristics of RO16.

name	CAS number	C.I. number	Formula	Molecular weight	$\lambda_{max}$
Reactive orange 16	12225-83-1	17754	C <sub>20</sub> H <sub>17</sub> N <sub>3</sub> Na <sub>2</sub> O <sub>11</sub> S <sub>3</sub>	617.54 g/mol	390

### Preparation of Nano size SiO<sub>2</sub>:

Tetraethoxysilane (TEOS) as a precursor was used. To fasten the hydrolysis reaction, ammonia as the catalytic systems was added [33]. After hydrolysis, nanoparticles of silica were formed. In order to control the size of nanospheres by adjusting the feed rate of raw materials a droplet generator was used. So, uniform spheres were produced while stirring the solution with a rapid stirring motor. The sample was centrifuged and washed and then kept on room temperature for a day. Afterwards they were dried in 110°C for 24 hours.

### Preparation of PANi/NS nanocomposite:

orange 16 ( $\lambda_{max}$ =390). Other equipment were UV-Vis spectrophotometer (Jenway model 6505), pH meter (Jenway model 3510), Scanning electronic microscope (LEO 440i, Leo Electron Microscopy, Cambridge, England), Transmission electronic microscope (Philips, CM/20, Netherlands). Fourier transform infrared (FT-IR) spectrometer (Shimadzu model 4100, Japan) and shaker bath equipped with thermostat (SDL-D403/1-3) operated at 100 rpm.

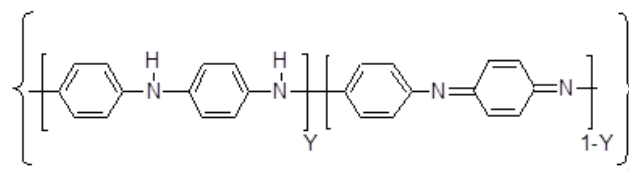


**Figure 9:** Structure of polyaniline (PANi) in various oxidation states.

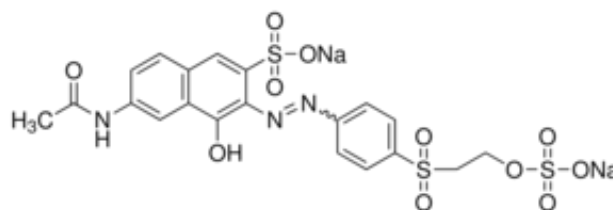


**Figure 10:** The chemical structure of RO16.

For preparation of PANi/NS nanocomposite, 1 g KIO<sub>3</sub> was added to 100 mL sulfuric acid (1 M) and then a uniform solution was resulted by using magnetic mixer. After 10 min, 1 g NS and 0.2 g CTAB were added to the solution and after 20 min, 1 mL fresh distilled aniline monomer was added to the stirred solution. The reaction was carried out for 5 h at room temperature. PANi/NS nanocomposite particles were separated from the reaction media and rinsed several times with deionized water and acetone and dried at 60 °C temperature in an oven for 24 h and stored in a desiccator for subsequent use.

### Batch adsorption experiment:

Batch experiments were conducted to investigate the parametric effects of adsorbent dose, adsorption time and pH for RO16 adsorption on the PANi/NS

nanocomposite. RO16 samples were prepared by dissolving a known quantity of dye in distilled water and used as a stock solution and diluted to the required initial concentration. 100 ml of RO16 solution of known concentration ( $C_0$ ) was taken in a 250 ml conical flask with a required amount of adsorbent and was shaken for different time duration in a shaker at different pH and Temperature. At the end of the process, the adsorbent was separated by centrifuging at 4000 rpm in 20 min. The amount of RO 16 in the solution before and after adsorption process was measured by UV-Vis spectrophotometer (Jenway model 6505).

The quantity of dye adsorbed on nylon6 samples at equilibrium were calculated using the following Eq. (7):

$$q_e = \frac{(C_0 - C_e)V}{W}$$

(7)

Where,  $q_e$  is the quantity of dye adsorbed on adsorbent (mg/g) at equilibrium,  $C_0$  and  $C_e$  are the initial and equilibrium dye concentrations (mg/l), respectively.  $V$  is the volume of dye bath (l) and  $W$  is the weight of adsorbent (PAni/NS) (g).

## References

- [1] Aksu, Z., *Pro. BioChem.* **2005**, *40*, 997.
- [2] Mezohegyi, G.; Kolodkin, A.; Castro, U. I.; Bengoa, C.; Stuber, F.; Font, J.; Fabregat, A.; Fortuny, A., *Indust. Eng. Chem. Res.* **2007**, *46*, 6788.
- [3] Dizge, N.; Aydiner, C.; Demirbas, E.; Kobya, M.; Kara, S., *J. Hazard. Mat.* **2008**, *150*, 737.
- [4] Garg, V. K.; Gupta, R.; Yadav, A. B.; Kumar, R., *Biores. Tech.* **2003**, *89*, 121.
- [5] Kannan, N.; Meenakshisundaram, M., *Wat. Air. Soi. Poll.* **2002**, *138*, 289.
- [6] Kadirvelu, K.; Palanival, M.; Kalpana, R.; Rajeswari, S., *Biores. Tech.* **2000**, *74*, 263.
- [7] Gupta, V. K.; Mittal, A.; Krishnan, L.; Gajbe, V., *Sep. Pur. Tech.* **2004**, *40*, 87.
- [8] Mittal, A.; Kurup, L.; Gupta, V. K., *J. Hazard. Mat.* **2005**, *117*, 171.
- [9] Javadian, H.; Ghorbani, F.; Tayebi, H. A.; Asl, S.H., *Arab. J. Chem.* **2013**, *8*, 837.
- [10] Shafiabadi, M.; Dashti, A.; Tayebi, H. A., *Syn. Met.* **2016**, *212*, 154.
- [11] Zareyee, D.; Tayebi, H. A.; Javadi, S.H., *Iran. J. Org. Chem.* **2012**, *4*, 799.
- [12] Zeng, X. R.; Ko, T. M., *Poly.* **1998**, *39*, 1187.
- [13] Ansari, R.; Khoshbakht Fahim, N.; Fallah Delavar, A., *Open. Pro. Chem. J.* **2009**, *2*, 1.
- [14] Kang, E. T.; Neoh, K. G.; Tan, K. L., *Prog. Poly. Sci.* **1998**, *23*, 277.
- [15] Li, X. G.; Li, A.; Huang, M. R., *Chem. A. Euro. J.* **2008**, *14*, 10309.
- [16] Gospodinova, N.; Terlemezyan, L., *Prog. Poly. Sci.* **1998**, *23*, 1443.
- [17] Huang, W. S.; Humphrey, B. D.; MacDiarmid, A.G., *J. Chem. Soc.* **1986**, *82*, 2385.
- [18] Sabatkova, Z.; Safarikova, M.; Safarik, I., *Biochem. Eng. J.* **2008**, *40*, 542.
- [19] Becker, J. S.; Thomas, O. R. T.; Franzreb, M., *Sep. Pur. Tech.* **2009**, *65*(1), 46.
- [20] Ma, Z.; Guan, Y.; Liu, H., *J. Mag. Mag. Mat.* **2006**, *301*, 469.
- [21] Zargar, B.; Parham, H.; Hatamie, A., *Talanta*, **2009**, *77*, 1328.
- [22] Gong, J. L.; Wang, B.; Zeng, G. M.; Yang, C. P.; Niu, C. G.; Niu, Q. Y.; Zhou, W. J.; Liang, Y., *J. Hazard. Mat.* **2009**, *164*, 1517.
- [23] Afkhami, A.; Saber-Tehrani, M.; Bagheri, H., *J. Hazard. Mat.* **2010**, *181*, 836.
- [24] Afkhami, A.; Saber-Tehrani, M.; Bagheri, H.; Madrakian, T., *Micro. Acta.* **2011**, *172*, 125.
- [25] Huang, C.; and Hu, B., *Spec. Acta.* **2008**, *63*, 437.
- [26] Afkhami, A.; Norooz-Asl, R., *Colloi. Sur. A: Phys. Eng. Asp.* **2009**, *346*, 52.
- [27] Afkhami, A.; Moosavi, R., *J. Hazard. Mat.* **2010**, *174*, 398.
- [28] Afkhami, A.; Moosavi, R.; Madrakian, T., *Talanta*, **2010**, *82*, 785.
- [29] White, B. R.; Stackhouse, B. T.; Holcombe, J. A., *J. Hazard. Mat.* **2009**, *161*, 848.
- [30] Tayebi, H. A.; Dalirandeh, Z.; Shokuhi Rad; A.; Mirabi; A. Binaeian, E., *Des. Wat. Treat.* **2016**, *1*.
- [31] Premaratne, W.A.P.J.; Priyadarshana, W.M.G.I.; Gunawardena, S. H. P.; De Alwis, A. A. P., *J. Sci. Uni. Kel.* **2013**, *8*, 33.
- [32] Tayebi, H. A.; Yazdanshenas, M. E.; Rashidi, A.; Khajavi, R.; Montazer, M., *J. Eng. Fab. Fib.* **2015**, *10*, 1.
- [33] Stoeber W.; Fink A.; Bohn E., *J. Coll. Int. Sci.* **1968**, *26*, 62.